

# Design and Performance of Liquid Xenon Detectors for PET

P. Amaudruz<sup>1</sup>, D. Bryman<sup>2</sup>, L. Kurchaninov<sup>1</sup>, P. Lu<sup>2</sup>, C. Marshall<sup>1</sup>, J. P. Martin<sup>3</sup>, A. Muennich<sup>1\*</sup>, F. Retiere<sup>1</sup>, A. Sher<sup>1</sup>, V. Sossi<sup>2</sup>

**Abstract**—We have developed a concept for a micro-PET detector that takes advantage of the improved performances achieved by measuring light and charge in Liquid Xenon. One sector was built and testing is in progress. The good performance in terms of efficiency and image quality of a LXe PET compared to a crystal based system has been shown in simulations.

## I. INTRODUCTION

**T**HIS work is aimed at studying the interactions of 511 keV photons in liquid xenon (LXe) detectors for applications to positron emission tomography (PET). The advantages of LXe for PET compared to currently used methods include improved energy resolution ( $< 10\%$  FWHM) by combining information from measuring the ionization as well as the scintillation light. This approach also allows for a 3-D sub-mm spatial resolution eliminating parallax errors. Because Compton interactions are more frequent than photoelectric interactions in LXe, this technology requires Compton event reconstruction but it also provides an additional means of rejecting background. The LXe detector can cover a large area using just one electrode plane and therefore reach a high sensitivity (70%) at relatively low cost. LXe also provides a high photon yield of  $68 \gamma/\text{keV}$  and a fast decay time of 2.2 ns which makes sub-ns time resolution possible. The count rate capability is estimated to be  $10^5/(\text{s cm}^2)$ .

## II. PROOF OF PRINCIPLE

A small test chamber ( $3 \times 3 \times 3 \text{ cm}^3$ ) was constructed to measure light and charge signals. An electric drift field was applied between the cathode and the shielding grid located near the anode charge collection plane as shown in Fig. 1. Two Advanced Photonics Inc. Large Area Avalanche Photodiodes (LAAPD) [1] were used to detect the scintillation light viewing a solid angle of 12%. Charge was collected on a central 1 cm diameter electrode or on an outer surrounding electrode. The 511 keV photons emitted by a  $^{22}\text{Na}$  source entered the test chamber (along the z axis) through the cathode plane and coincidences with an external NaI detector were studied. To study the energy resolution we focused on the central region of the test chamber. Fig. 2 shows the energy distributions observed for charge, light and the combination of both. The lower left plot shows the linear anti-correlation between the

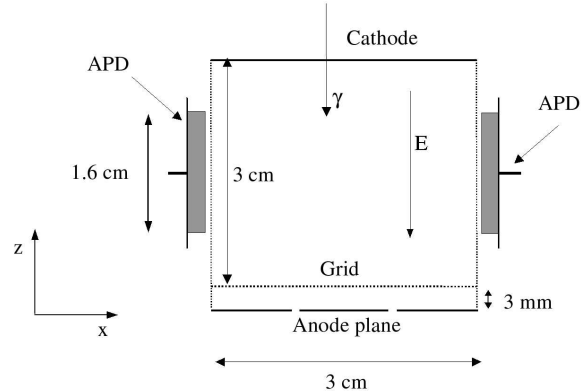


Fig. 1. Small TPC prototype to demonstrate simultaneous measurement of light and charge.

light and charge measurement and the axis of the ellipse. The upper left plot shows the charge spectrum collected on the anode which is equal to a projection of the correlation along the light axis. In the upper right plot the projection of the correlation along the charge axis can be seen, giving the spectrum of the collected light. The lower right plot demonstrates the improved energy resolution of the combined spectrum: The 511 keV region ellipse of the charge-light anti-correlation is used to obtain the ellipse axis along which the spectrum is projected. With this setup we measured 11.4% energy resolution (rms) for scintillation light and 5.6% (rms) for ionization. Making use of the anti-correlation between these two signals we achieved a combined energy resolution of 3.9% (rms) corresponding to 9.2% FWHM.

## III. DESIGN FOR A MICRO-PET DETECTOR

Our micro-PET detector concept is shown in Fig. 3. We foresee dividing the PET detector ring in 12 identical liquid Xenon filled trapezoidal sectors. The scintillation light is measured by 32 LAAPDs. The charge measurement is achieved by using a time projection chamber (TPC) which is based on the design for the LXeGRIT detector [2]. Electrons produced in the liquid drift to the anode plane under an applied electric field. The anode plane is segmented into 96 strips separated by 1.1 mm for position reconstruction. Above the anode plane, 96 induction wires are strung perpendicular to the anode strips providing the second position coordinate. The maximum drift length is 12 cm. The position along the drift direction is reconstructed by measuring the time between the light flash

\* corresponding author, contact: muennich@triumf.ca

<sup>1</sup>TRIUMF, 4004 Wesbrook Mall, Vancouver, BC, V6T 2A3

<sup>2</sup>The University of British Columbia, 2329 West Mall Vancouver, BC Canada V6T 1Z4

<sup>3</sup>The University of Montreal, Montreal, PQ, Canada

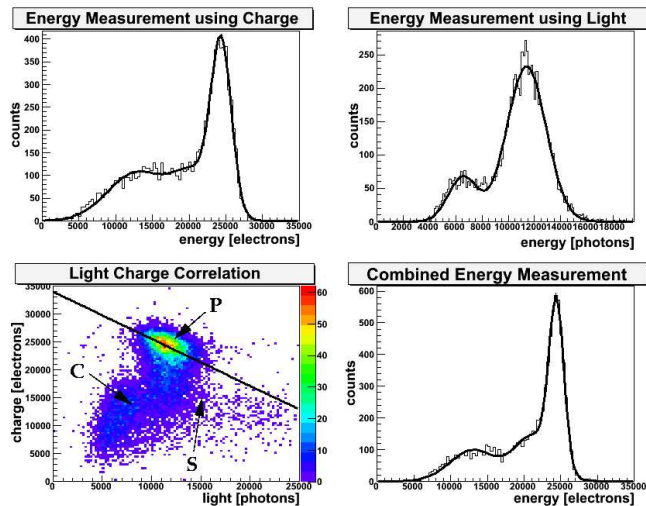


Fig. 2. The observed charge spectrum (upper left plot), light spectrum (upper right plot), correlation between light and charge signals (lower left plot), and combined spectrum using the correlation (lower right plot) for 511 keV photons with a drift field of 2.66 kV/cm. The data points in the correlation plot that are not part of the Compton (C) or the photoelectric peak (P) are due to photons that scattered outside the detector (S).

and the charge arrival on the anode plane, knowing the drift velocity. The electrons can take up to 50  $\mu$ s to reach the anode plane. Hence, when the interaction rate is larger than about 100 kHz, the location of the interaction must be reconstructed with the light only with a precision of about 1 cm in order to ensure proper matching between scintillation and ionization signals.

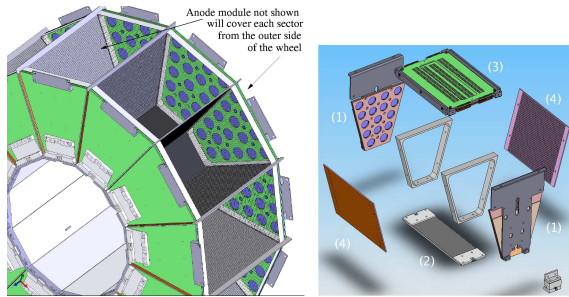


Fig. 3. Left: The LXe PET ring concept. Scintillation light and charge are measured in each of the 12 modules consisting of a LXe time projection chamber viewed by avalanche photodiodes. Right: Parts of one sector: APD Module(1), Cathode(2), Anode Module(3), Field Cage(4)

One sector prototype has been designed and all parts built. Fig. 4 shows a partly assembled sector mounted onto the cryostat flange and a view inside the sector with field-strips, anode and APD module visible.

#### IV. POTENTIAL OF LXE DEMONSTRATED WITH SIMULATIONS

GEANT4 [3] has been used to simulate a Micro-PET system with 14 cm inner diameter, 38 cm outer diameter and 8 cm in length. The dimension were chosen to match the commercially available Focus120 [4] to compare results. In the simulation

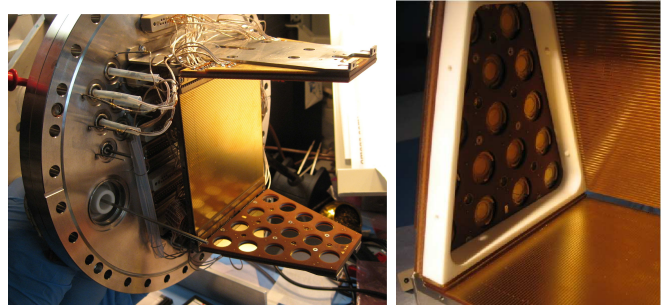


Fig. 4. Prototype of a sector for a LXe PET detector. In the left picture parts of the sector are shown mounted onto the flange that holds the detector within the cryostat. The right picture shows a view inside the sector looking onto the APD module (no APDs mounted yet) and the strips of the field cage as well as the anode module.

the positron range was included whereas the non-collinearity was not. An energy resolution of 9%, a position resolution of 1mm (both FWHM) and a dead time of 500 ns were assumed. The coincidence window used is 6 ns. Compton reconstruction was used to get the first point of interaction of each 511keV photon and to suppress backgrounds. Table I shows a comparison between the sensitivity for a point source in the center of the field of view for the LXePET and values published for the Focus120 in [4]. A better sensitivity is achieved with the LXe system than with the crystal based Focus120. This is mainly due to more active volume and less inactive material than can absorb or scatter photons and a better timing resolution.

TABLE I  
SENSITIVITY FOR A POINT SOURCE SIMULATED FOR LXe AND MEASURED FOR FOCUS120.

Energy Window [keV]	LXe [%]	Focus120[%]
250	10.2	6.7
350	9.3	3.8

One indicator used to qualify image quality is the Noise Equivalent Count Rate (NECR). Fig. 5 shows the simulated result for the LXe system using a NEMA-like rat sized phantom. Peak values for the NECR of the Focus120 are 230(200) kcps for and energy threshold of 250(350)keV.

A visual comparison of the reconstructed image of a Dorenzo phantom is shown in Fig. 6. A simple reconstruction using Filter-Back Projection was used causing some artifacts in the Focus120 picture due to the limited binning size given by the crystals. The emphasis here is on the comparison of the resolution and not the image quality. The small rods with 1 mm diameter are still distinguishable with the LXePET. Given that the positron drift range is 1mm or higher depending on the isotopes, the LXe detector resolution is limited primarily by the positron range in this simulation.

#### V. CONCLUSION

A small liquid xenon TPC has been shown to give excellent energy resolution (<10% FWHM) by combining ionization charge and scintillation light signals observed with avalanche

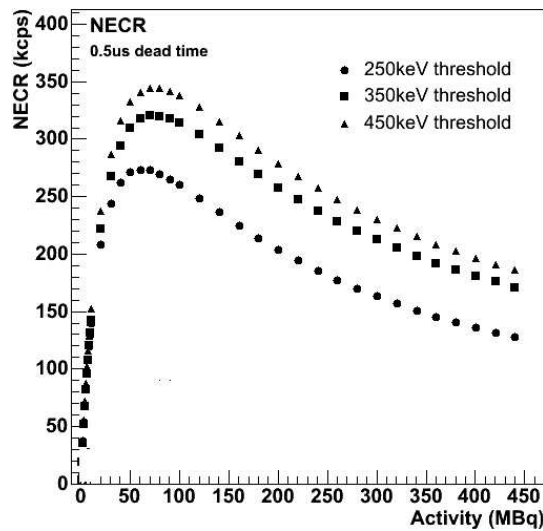


Fig. 5. NECR for LXePET in dependence on the source activity for different energy thresholds

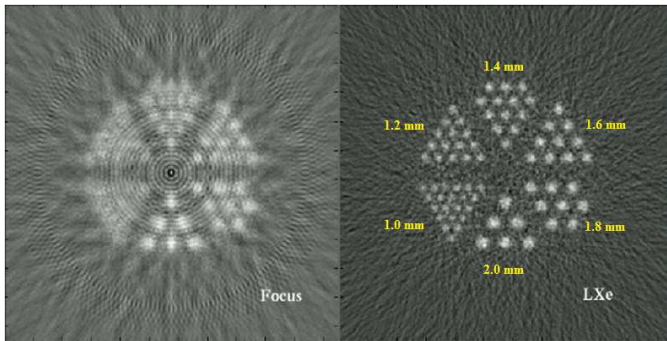


Fig. 6. Reconstructed image of a Dorenzo phantom for both detector systems.

photodiodes. We are presently designing and building a prototype of one sector for a Micro-PET scanner. The design of full Micro-PET system in progress. The next step is to operate and test the first sector prototype. Following that a second sector will be built and operated in coincidence for PET measurements within a cryostat designed for a full PET ring.

This work was supported by TRIUMF and the Canada Foundation for Innovation.

#### REFERENCES

- [1] V.N. Solovov *et al.*, *Study of large area avalanche photodiode for detecting liquid xenon scintillation*, IEEE Transactions on Nuclear Science, Vol.47, No.4, pp.1307-1310, 2000
- [2] E. Aprile *et al.*, *Compton Imaging of MeV Gamma-Rays with the Liquid Xenon Gamma-Ray Imaging Telescope (LXeGRIT)*, submitted to Nucl. Instr. and Meth. A, 2008
- [3] S. Agostinelli *et al.* [GEANT4 Collaboration], *GEANT4: A simulation toolkit*, Nucl. Instrum. Meth. A 506, 250 (2003).
- [4] Jin Su Kim *et al.*, *Performance Measurement of the microPET Focus 120 Scanner*, Journal of Nuclear Medicine Vol. 48 No. 9 1527-1535, 2007